JSCAI
The official journal of the Society for Cardiovascular Angiography & Interventions

Original Research

Implementing Patient Protection Radiation Dose Alerts for Pediatric Cardiac Catheterization Examinations

Elanchezhian Somasundaram, PhD [a,b], Russel Hirsch, MD [a,b], Samuel L. Brady, MS, PhD [a,b], Karen S. Minsterman, RN [a], Keith J. Strauss, MSc [a,b,*]

[a] Cincinnati Children's Hospital Medical Center, Cincinnati, Ohio; [b] University of Cincinnati College of Medicine, Cincinnati, Ohio

ABSTRACT

Background: Advancements in cardiac catheterization have improved survival for pediatric congenital heart disease patients, but the associated ionizing radiation risks necessitate ethical consideration.

Methods: This study presents an empirical model, developed from 3131 unique pediatric procedures, to establish alert levels based on a patient's lateral thickness of the thorax for various procedural categories during diagnostic or interventional cardiac catheterization. The model uses linear regression of logarithmic reference air kinetic energy released per unit mass (KERMA) and air KERMA area product, also referred to as dose area product, to set alert levels at the top 95% and 99% of patient data.

Results: Coefficients of the regression fits are provided for diagnostic and interventional procedural groups and fluoroscopic plane allowing any facility to scale the results of this study's single facility data to model their practice's unique procedural dose levels.

Conclusions: The proposed method allows institutions to tailor dose alert levels to their specific pediatric populations to reduce overexposure events.

Introduction

The incidence of moderate to severe pediatric congenital heart disease (CHD) was reported to be 6 and 19 out of 1000 individuals, respectively.[1,2] Mortality rates for CHD have declined since the early 1990s, to around 1 per 100,000 in the US and 4 per 100,000 worldwide, because of advancements in surgical and treatment procedures.[2] With decreasing mortality rates, pediatric patients with CHD experience longer life expectancy, necessitating extended follow-up care.

Although the treatment and follow-up care for CHD is predominantly dependent on noninvasive studies (primarily echocardiography), approximately 10% of pediatric patients require cardiac catheterization for better hemodynamic assessment and therapeutic intervention, with the attendant exposure to ionizing radiation.[3,4] A study found that the median cumulative effective dose for children with CHD from all ionizing radiation imaging modalities is 2.7 mSv, ranging from 0.1 to 76.9 mSv (5th to 95th percentile), with cardiac catheterization procedures contributing 60% of the total radiation burden.[3] Over 85% of children with CHD now survive into adulthood,[5] requiring ongoing follow-up with diagnostic and therapeutic studies that increase their total radiation dose. Follow-up imaging doses range from 0.03 mSv for chest radiography to 18 mSv for a gated computed tomography angiography,[3] while therapeutic procedures range from 0.1 mSv for diagnostic electrophysiology studies to over 100 mSv for transcatheter aortic valve replacement procedures.[4]

Advancements in imaging technology and procedures in recent years[6–10] have significantly contributed to reducing patient population doses in cardiac catheterization laboratories (CCL). However, with increasing survival, a broader range of interventional/percutaneous procedures available for palliation, and the need for frequent repeat catheterizations in some circumstances, a more targeted approach to the comprehensive understanding of patient exposures to ionizing radiation across the pediatric spectrum is needed.

Radiation dose index monitoring (RDIM) software is a valuable tool that can create alerts when patient doses have exceeded threshold levels for specific types of examinations as a function of patient size.[11–13] This software enables the collection and analysis of radiation output data, eg, reference air KERMA (RAK), air kinetic energy released

Abbreviations: DAP, dose area product; Diagnostic-H, diagnostic studies at high dose; Diagnostic-L, diagnostic studies at low dose; Intervention-C, interventional studies with high complexity; Intervention-M, interventional studies with medium complexity; Intervention-S, interventional studies with simple complexity; ISO, isocenter; KERMA, kinetic energy released per unit mass; LAT, lateral thickness; RAK, reference air KERMA.

Keywords: cardiac catheterization; patient dose; pediatric; quality assurance; safety.

* Corresponding author: keith.strauss@cchmc.org (K.J. Strauss).

https://doi.org/10.1016/j.jscai.2024.102292
Received 15 April 2024; Received in revised form 21 July 2024; Accepted 19 August 2024; Available online 7 September 2024

Table 1. Correlation of patient age, weight, height, and body mass index to the lateral thickness of the thorax.

Lateral thorax, cm	Ave age, y	Ave weight, kg	Ave height, cm	Ave BMI[a], kg/m^2
16.3	0	5.1	56	16.3
16.7	0.5	7.7	66	17.7
17.1	1	11.2	81	17.1
18.1	2	13.6	91	16.4
19	3	16	98	16.7
19.9	4	18.3	105	16.3
20.8	5	21	112	16.7
21.7	6	23.8	118	16.8
22.7	7	27.5	125	17.6
23.6	8	31.5	131	18.4
24.5	9	35.2	136	19.0
25.4	10	41	142	20.3
26.3	11	47.3	150	21.0
27.3	12	50.9	155	21.2
28.2	13	58.7	160	21.6
29.1	14	63.1	165	22.9
30	15	67.6	166	24.5
30.9	16	68.5	168	24.3
31.8	17	72.5	169	25.4
32.8	18	74	169	25.9
33.7	19	75.5	169	26.4
34.6	20	78.8	169	27.6

Correlation of lateral thorax thickness and average patient age.[22]
Correlation between average patient weight and average height to patient average age.[23]
BMI, body mass index.
[a] Average BMI = patient average weight/(patient average height).[2]

per unit mass (KERMA) area product also referred to as dose area product (DAP), total fluoroscopy time, and more. Tracking of dose metrics is linked to patient population demographics (eg, adult vs pediatric, age, weight, body mass index [BMI], the lateral thickness (LAT) of the patient's thorax, etc.), diagnostic or therapeutic procedure type, and equipment specifications. When RDIM software is equipped with appropriate dose thresholds, an unusually high patient dose for a given examination and patient size can trigger an alert level and activate an investigation and potential corrective actions. An alert level does not imply a maximum allowed dose; it is simply a dose trigger that could be exceeded depending on the complexity of the examination. Also, alert levels track only patient dose; this aspect of a quality assurance program does not evaluate image quality nor validate it.

Recent initial benchmark dose data[14] has been established for some adult cardiac catheterization procedures to guide the development of adult alert levels. Limited published dose data for pediatric cardiac catheterizations exists,[3,15–21] but its value is limited. Those data are more than a decade old and do not model current, reduced patient doses due to technological improvement in fluoroscopic imaging equipment. Further, it does not provide dose data as a function of the pediatric patient's size.

In this study, diagnostic and therapeutic procedures from a major pediatric medical center with a large pediatric and congenital heart service were analyzed as a function of patient size to establish RAK and DAP alert levels in a pediatric CCL. Additionally, we created a methodology for generalizing the RAK and DAP alert level threshold data of this study to enable any facility, whether pediatric or adult-focused, to scale this study's data to model its population's RAK and DAP values.

Materials and methods

Data collection

This retrospective study anonymized all patient data and was compliant with the Health Insurance Portability and Accountability Act. The institutional review board waived the need for consent for this retrospective study. The LAT of each patient's thorax at the level of the heart (distance from the entrance skin surface to exit skin surface of the lateral projection through the supine patient on the gantry couch in a hospital gown) was measured to the nearest whole centimeter using manual calipers to estimate the path lengths traversed by the primary x-rays. Anteroposterior thicknesses measured with a manual caliper can be difficult to obtain if the patient support is not flat. If the anteroposterior thickness of the chest at the level of the heart was needed, it was derived from Kleinman et al[22] as matched to the lateral measured thickness. As opposed to patient age, the thickness of the thorax is the preferred correlation metric to characterize the RAK and DAP cardiac catheterization alert levels because the LAT of the thorax of the largest 3-year-old is the same size as the smallest 17-year-old.[22] Table 1[22,23] lists the average age,[22] weight,[23] height,[23] and BMI that corresponds to the LAT of the thorax when this thickness was unknown. Measured LAT of the patient's thorax and the digital imaging and communications in medicine Radiation Dose Structured Report data for each examination were recorded in an RDIM database (Clinical Microsystems Corporation) from January 1, 2016, through March 31, 2022. Patients included in this study ranged from newborns to 21-year-old patients; the study included 3131 examinations. The basic configuration of the 3 biplane interventional fluoroscopes, which determined the delivered patient dose rates during the 6-year study, remained unchanged.

Patient dose indices

The air KERMA displayed by the fluoroscope was the first dose index analyzed. This index, (air KERMA without backscatter at interventional reference point) was defined as RAK, in units of mGy, without backscatter at the interventional reference point (IRP).[24] The IRP was defined for an average-sized adult, ie, 15 cm from the isocenter (ISO) of the fluoroscope's gantry toward the focal spot. Because the average pediatric patient's entrance skin plane was seldom at the IRP, the displayed RAK stored in the Radiation Dose Structured Report was corrected by applying the inverse square law using Equation 1 as follows:

$$ISC = \left[\frac{IRP}{ISO - \frac{AP+LAT}{4}}\right]^2 \qquad \text{Equation 1}$$

where ISC is the inverse square law correction factor, IRP is the interventional reference point (see Table 2),[21,24] ISO is the isocenter

Table 2. Basic specifications of each type of fluoroscope in the study.

Type	Quantity	Manufacturer	Model	Isocenter, cm[a]	Interventional reference points, cm[b]
FGI	2	Philips Healthcare Solutions	Allura Xper FD10 with Clarity Image Processing: Biplane unit	Frontal plane: 76.5 cm Lateral plane: 76.6 cm	Frontal plane: 61.5 cm Lateral plane: 61.6 cm
FGI	1	Philips Healthcare Solutions	Allura Xper FD20 with Clarity Image Processing: Biplane unit	Frontal Plane: 81 cm Lateral Plane: 76.6 cm	Frontal plane: 66 cm Lateral plane: 61.6 cm

FGI, fluoroscopically guided interventional unit.
[a] Isocenter is the distance from the focal spot to the point of rotation of the gantry of the fluoroscope. [b] Interventional reference point is the distance from the focal spot to a point 15 cm back from the isocenter toward the x-ray tube.[21,24]

Table 3. Examination descriptions within each of the 5 patient groupings.

Group	Examination descriptions
Diagnostic-L	Biopsy post heart transplant, right heart catheterization
	Right and left heart catheterization with extra hemodynamic investigations
	Right and left heart catheterization
Diagnostic-H	Biopsy post heart transplant, right and left heart catheterization with coronary angiography.
	Left heart catheterization with coronary angiography
	Right and left heart catheterization with heart failure management device implant
	Angiography of head and neck vessels
Intervention-C	All stent interventional procedures
	Transcatheter valve implants
Intervention-M	Multiple collateral vessel closure interventional procedures
	All balloon angioplasty interventional procedures
Intervention-S	Limited collateral vessel closure interventional procedures
	Atrial septal defect closure interventional procedures
	Patent ductus arteriosus closure interventional procedures
	Balloon valvuloplasty interventional procedures

Diagnostic-H, diagnostic studies at high dose; Diagnostic-L, diagnostic studies at low dose; Intervention-C, interventional studies with complex complexity; Intervention-M, interventional studies with medium complexity; Intervention-S, interventional studies with simple complexity.

of the gantry of the fluoroscope (see Table 2), AP is the anteroposterior thickness of thorax measured in cm, and LAT is the lateral thickness of thorax measured in cm. The quantity (AP + LAT)/4 calculates the average patient radius during the examination, which results in RAK at the entrance skin plane of the pediatric patient used in this study. The inverse square law correction factor to RAK assumes that the center of the heart is placed at the ISO of the gantry of the fluoroscope.

The second displayed dose index analyzed was DAP (in units of mGy·cm^2). This dose index was defined as the product RAK and the area of the x-ray field at the IRP. The DAP of interest in this study was the product of RAK and the area of the x-ray field at the entrance skin plane of the patient. Correction factors to cumulative values of both RAK and DAP were also calculated annually from radiation output measurements compared to displayed values of cumulative RAK and DAP at the interventional reference point[21,24] to reduce measurement errors of the displayed RAK and DAP to better than ± 5%.

Although the use of RAK for alert levels is preferred, DAP is also reported because it is more commonly used in cardiology. Because DAP is independent of the distance between the focal spot and the entrance plane of the patient, the inverse square law correction factor for different-sized patients does not apply to DAP.

Specifications of the 3 utilized fluoroscopes are provided in Table 2.

Clinical procedure groupings

Patient data were sorted into 5 groups of CCL procedures labeled as follows: diagnostic studies at low dose (Diagnostic-L), diagnostic studies at high dose (Diagnostic-H), interventional studies with simple complexity (Intervention-S), interventional studies with medium complexity (Intervention-M), and interventional studies with high complexity (Intervention-C). For the 2 diagnostic groups, and the 3 intervention groups, procedures were categorized based on frontal plane RAK in consultation with an interventional cardiologist (R.H.) who has 24 years of experience performing pediatric cardiac catheterizations. After data collection, the average frontal plane RAK for a specific clinical group independent of patient size resulted in some of the clinical examination types reclassifying between low and high for the diagnostic studies and between S, M, and C for interventional studies. This second adjustment within the 5 groups reduced the range of RAK and DAP within each group and increased the difference in the average RAK and DAP values between the 5 groupings. Table 3 lists the examination descriptions grouped together to create the 5 different patient groupings.

Validation of 5 clinical procedure groupings

To validate the procedure groupings, post hoc analysis of variance models with procedure group and patient size as predictor variables, and logarithmic dose (DAP and RAK, individually) as the response variable were modeled using emmeans[25] package in R.[26] Mean dose (intercept) and slope comparisons were performed between each group independently for planes A and B using the "lsmeans" and "lstrends" functions. The *P* values from the comparisons at the 0.95 confidence level were calculated.

Trigger levels for RAK and DAP

Based on the log-transformed simple linear fit equation developed for general fluoroscopy RAK alert levels as a function of patient size in our previous work,[27] the equation for calculating RAK and DAP alert levels at different upper quantile prediction levels[28] (for 50%, 90%, and 98%) for the CCL were derived. The coefficients of the linear fits of these levels can be used to set desired dose alert levels $\widehat{D}$ at different values of α using the equation below:

Table 4. Procedure-wise patient and dose metrics for the study dataset.

Group	Imaging Plane	N	Age, y	Lateral size, cm	RAK[a], mGy	DAP[b], mGy·cm^2
Diagnostic-L	Frontal	1044	11.0 ± 9.7	24.3 ± 8.6	9.3 ± 17.4	2359 ± 5301
Diagnostic-H	Frontal	472	11.5 ± 7.6	25.4 ± 7.3	22.3 ± 34.9	5167 ± 9244
Intervention-S	Frontal	548	7.2 ± 10.3	20.2 ± 8.3	13.5 ± 38.9	3138 ± 7526
Intervention-M	Frontal	492	5.9 ± 8.4	19.2 ± 6.9	30.4 ± 61.4	7370 ± 18,978
Intervention-C	Frontal	586	8.9 ± 11.4	21.7 ± 8.4	62.1± 164.7	14,839 ± 36,120
Diagnostic-L	Lateral	888	10.7 ± 9.7	24.0 ± 8.4	17.3 ± 42.0	2945 ± 8985
Diagnostic-H	Lateral	450	11.9 ± 7.4	25.8 ± 7.1	43.8 ± 72.2	6499 ± 12,268
Intervention-S	Lateral	586	6.8 ± 10.1	19.8 ± 8.1	41.3 ± 195.9	5900 ± 23,420
Intervention-M	Lateral	474	6.1 ± 8.5	19.3 ± 7.0	41.9 ± 135.0	6190 ± 25,128
Intervention-C	Lateral	590	8.4 ± 10.4	21.4 ± 8.3	74.4 ± 163.3	12,499 ± 31,581

All the values in the Age, Lateral size, RAK, and DAP columns are mean ± SD.
Diagnostic-H, diagnostic studies at high dose; Diagnostic-L, diagnostic studies at low dose; Intervention-C, interventional studies with complex complexity; Intervention-M, interventional studies with medium complexity; Intervention-S, interventional studies with simple complexity.
[a] RAK: air KERMA without backscatter at patient's entrance skin plane. [b] DAP: product of reference air KERMA and area of x-ray field at patient's entrance skin plane.

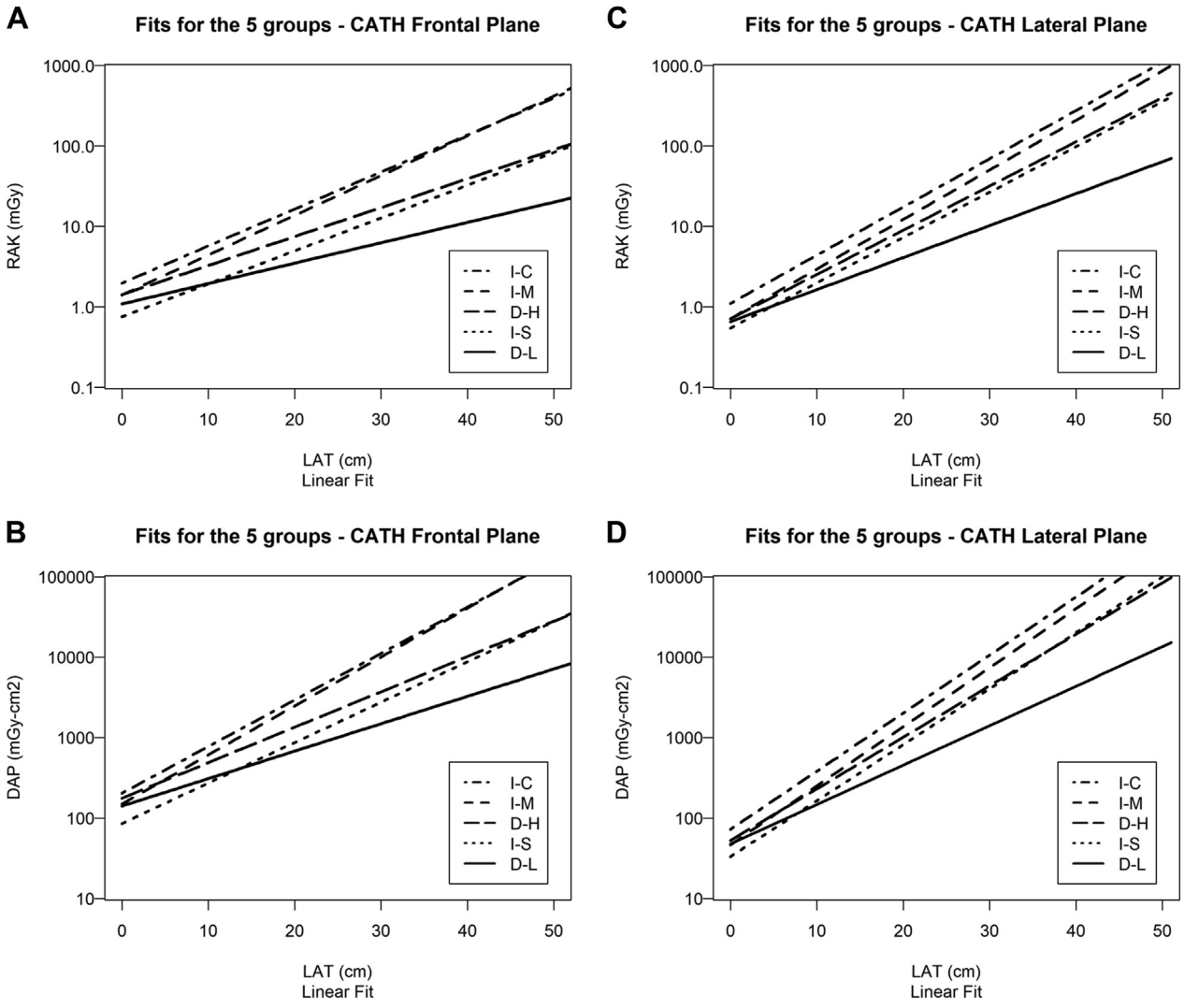

Figure 1.

Patient dose for 5 patient groups vs lateral thickness (LAT) of the patient's thorax. Log reference air KERMA (RAK) or log product of dose area product (DAP) of x-ray beam vs patient thorax LAT**:** (**A**) RAK for the frontal plane. (**B**) DAP for the frontal plane. (**C**) RAK for the lateral plane. (**D**) DAP for the lateral plane. Five patient groups: diagnostic studies at low dose (D-L), diagnostic studies at high dose (D-H), interventional studies with simple complexity (I-S), interventional studies with medium complexity (I-M), and interventional studies with high complexity (I-C). The LAT of the patient's thorax is the independent variable.

$$\widehat{D}_{\alpha}(x_{new}) = EXP(m \cdot x_{new} + \widehat{c} + s_{\alpha}) \qquad \text{Equation 2}$$

where x_{new} is the patient size in cm for a new patient, $\widehat{D}$ can be either RAK in mGy or DAP in mGy·cm^2 and separate coefficients (m, s_{α}, *and* $\widehat{c}$) for either dose measure are calculated for each procedure group and dose plane. m represents the average slope of the dose prediction fits as a function of patient size. s_{α} is calculated as the logarithm of the ratio between the mean dose to the trigger dose at level α for a given patient size. $\widehat{c}$ is the intercept value of each linear dose fit. $\widehat{c}$ may be calculated by any institution based on their unique average dose level (D_{avg}) for the institution's average-sized patient (x_{avg}) as follows:

$$\widehat{c} = \ln(D_{avg}) - m \cdot x_{avg} \qquad \text{Equation 3}$$

where D_{avg} is the institution's RAK or DAP, m and s_{α} are predetermined constants presented for each dose measure, procedure group, and dose plane based on the data samples from this study. The α values of 50%, 90%, and 98% corresponded to the levels above which 25%, 5%, and 1% of the expected dose values will occur based on the data samples collected in this study as a function of patient size ranging from 0 to 50 cm.

Application

The data collected in this study were used to create an empirical model to calculate an alert level RAK or DAP for a specific type of fluoroscopic examination and dose plane, summarized by Equations 2 and 3. To account for differences in mean dose level, between this study's results and those at other institutions, Equation 3 enables recalculation of $\widehat{c}$, the intercept of the fitted curve. When $\widehat{c}$ for a different institution is substituted into Equation 2, the resulting dose alert level will be scaled to account for the average RAK or DAP at that institution, provided an average RAK or DAP for a small sample of patients of the same size can be measured for their unique cardiac catheterization examinations.

Results

Patient examinations with RAK <1 mGy within Diagnostic-L and RAK <2 mGy within the other 4 categories were removed from the analysis

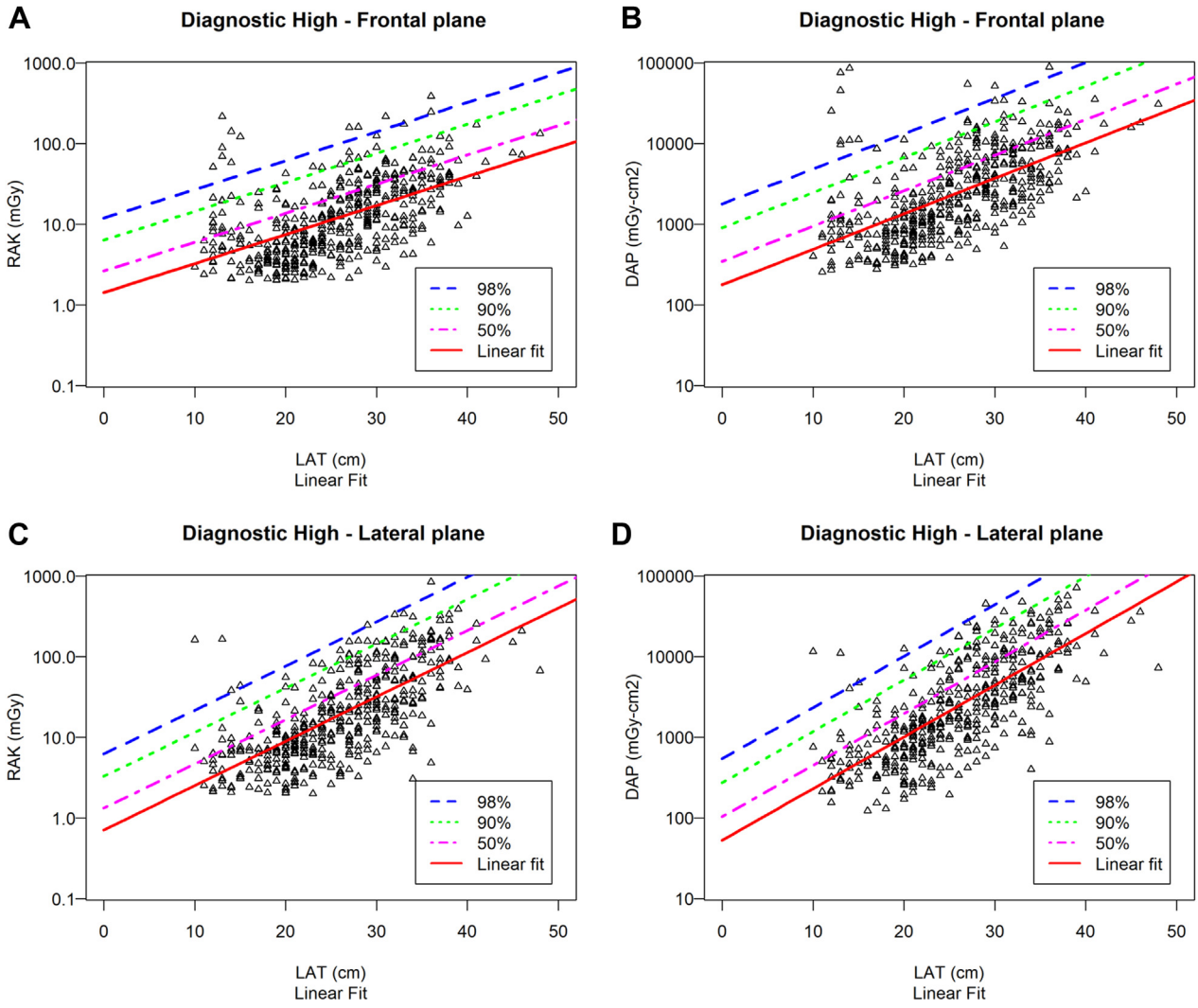

Figure 2.

Four levels of patient dose (diagnostic studies at high dose [Diagnostic-H or Diagnostic High]) vs lateral thickness (LAT) of the patient's thorax. Log reference air KERMA (RAK) or log of dose area product (DAP) of x-ray beam vs patient's thorax LAT. Diagnostic-H: (**A**) RAK for the frontal plane. (**B**) DAP for the frontal plane. (**C**) RAK for the lateral plane. (**D**) DAP for the lateral plane. The RAK and DAP were fit for 50%, 90%, and 98% upper prediction levels in addition to a linear fit. The LAT of the patient's thorax is the independent variable for both gantry planes.

of the data because these studies did not represent meaningful use of ionizing radiation in the procedure. The number of patient examinations remaining in this study for each clinical procedure and imaging plane, *N*, along with mean age, LAT thickness, RAK, and DAP are provided in Table 4.

Figure 1 shows the plots of the linear fits of patient RAK and DAP, for both imaging planes, as a function of patient LAT for each of the 5 cardiac catheterization clinical procedure groups. Example linear fits of the log-transformed RAK or DAP, are presented for 2 of the 5 clinical procedure groups, namely: Diagnostic-H (Figure 2) and Intervention-C (Central Illustration). The figures also include linear fits for the upper prediction intervals at 50%, 90%, and 98%, representing thresholds where 25%, 5%, and 1% of the patient data lie, respectively. These prediction levels set thresholds for RAK or DAP patient data, informing quality assurance alert levels using Equation 2 for any imaging plane.

Tables 5 and 6 show the coefficients for Equation 2 for RAK and DAP respectively; the coefficients for the frontal plane gantry are followed by those for the lateral plane. These tables enable institutions to calculate customized RAK or DAP alert levels for their cardiac catheterization patients using Equations 2 and 3. Doses at other facilities, larger or smaller than those in this study, lead to correspondingly larger or smaller intercepts $\hat{c}$ compared to Tables 5 and 6. Negative $\hat{c}$ values in both tables are not significant. Shifting the fitted curves lower due to smaller doses may result in $\hat{c}$ passing through 0 and becoming negative. However, a negative $\hat{c}$ does not imply a negative dose due to LAT exceeding 10 cm in the smallest patients.

Table 7 shows the results of the post hoc comparison between the dose groups for each procedure type (diagnostic and intervention). All 16 plotted intercepts are significantly different. The slopes for the 2 diagnostic catheterization levels differ significantly for both RAK and DAP, but this is not the case for the 3 interventional catheterization levels.

Discussion

This study uses pediatric RAK and DAP dose estimates correlated to the lateral thickness of the thorax, during cardiac catheterizations performed at a high-volume congenital heart center in a tertiary care pediatric institution. Four empirical fits of RAK and DAP, for each of the 5 examination groupings, are provided for the frontal and lateral planes of the fluoroscope. This methodology scales the RAK and DAP alert

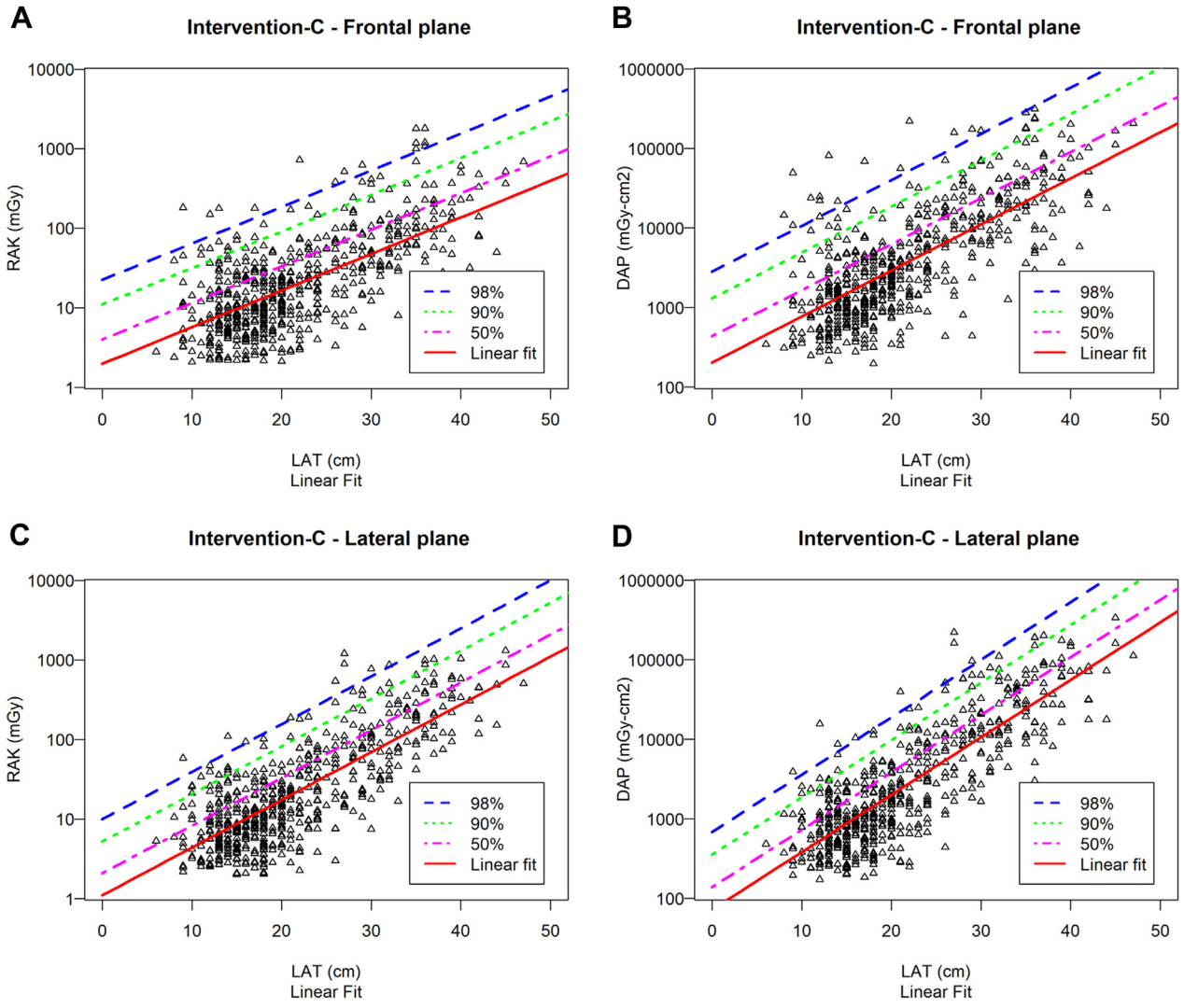

Central Illustration.

Four levels of patient dose (interventional studies with high complexity [Intervention-C]) vs lateral thickness (LAT) of the patient's thorax. Log reference air KERMA (RAK) or log product of dose area product (DAP) of x-ray beam vs patient's thorax LAT. Intervention-C: (**A**) RAK for the frontal plane. (**B**) DAP for the frontal plane. (**C**) RAK for the lateral plane. (**D**) DAP for the lateral plane. The RAK and DAP data were fit for 50%, 90%, and 98% upper prediction levels in addition to a linear fit. The LAT of the patient's thorax is the independent variable for both gantry planes.

Table 5. Coefficients for calculating RAK levels for each patient group.

Group	Plane	Slope, m	S_{50}	S_{90}	S_{98}	Intercept ($\hat{c}$)
Diagnostic-L	Frontal	0.059	0.645	1.573	2.226	0.086
Diagnostic-H	Frontal	0.084	0.596	1.456	2.063	0.354
Intervention-S	Frontal	0.095	0.605	1.476	2.09	–0.282
Intervention-M	Frontal	0.115	0.582	1.42	2.011	0.342
Intervention-C	Frontal	0.107	0.69	1.684	2.384	0.682
Diagnostic-L	Lateral	0.92	0.707	1.725	2.441	–0.420
Diagnostic-H	Lateral	0.128	0.606	1.481	2.098	–0.339
Intervention-S	Lateral	0.131	0.701	1.711	2.422	–0.607
Intervention-M	Lateral	0.143	0.598	1.46	2.067	–0.338
Intervention-C	Lateral	0.139	0.625	1.525	2.16	0.098

Diagnostic-H, diagnostic studies at high dose; Diagnostic-L, diagnostic studies at low dose; Intervention-C, interventional studies with complex complexity; Intervention-M, interventional studies with medium complexity; Intervention-S, interventional studies with simple complexity; RAK, reference air KERMA; S_{50}, 50% upper prediction level; S_{90}, 90% upper prediction level; S_{98}, 98% upper prediction level.

Table 6. Coefficients for calculating DAP levels for each patient group.

Group	Plane	Slope, m	S_{50}	S_{90}	S_{98}	Intercept ($\hat{c}$)
Diagnostic-L	Frontal	0.079	0.686	1.675	2.37	4.950
Diagnostic-H	Frontal	0.102	0.647	1.579	2.237	5.177
Intervention-S	Frontal	0.117	0.688	1.68	2.379	4.452
Intervention-M	Frontal	0.142	0.634	1.548	2.192	5.010
Intervention-C	Frontal	0.134	0.748	1.825	2.584	5.317
Diagnostic-L	Lateral	0.113	0.773	1.885	2.669	3.869
Diagnostic-H	Lateral	0.149	0.65	1.588	2.249	3.967
Intervention-S	Lateral	0.161	0.698	1.703	2.411	3.500
Intervention-M	Lateral	0.17	0.603	1.473	2.086	3.839
Intervention-C	Lateral	0.167	0.638	1.559	2.207	4.283

DAP, dose area product; Diagnostic-H, diagnostic studies at high dose; Diagnostic-L, diagnostic studies at low dose; Intervention-C, interventional studies with complex complexity; Intervention-M, interventional studies with medium complexity; Intervention-S, interventional studies with simple complexity; S_{50}, 50% upper prediction level; S_{90}, 90% upper prediction level; S_{98}, 98% upper prediction level.

Table 7. *P* values from comparing intercepts and slopes between dose groups at the 0.95 confidence level.

Procedure	Comparison	Dose	Frontal plane		Lateral plane	
			Intercept *P* value	Slope *P* value	Intercept *P* value	Slope *P* value
Diagnostic	Low-High	RAK	<.0001	.0004	<.0001	<.0001
Diagnostic	Low-High	DAP	<.0001	.0020	<.0001	<.0001
Intervention	S – M	RAK	<.0001	.0322	<.0001	.2822
Intervention	S – M	DAP	<.0001	.0134	<.0001	.5303
Intervention	S – C	RAK	<.0001	.1873	<.0001	.4484
Intervention	S – C	DAP	<.0001	.0478	<.0001	.6666
Intervention	M – C	RAK	.0070	.5604	<.0001	.8782
Intervention	M – C	DAP	.0264	.7037	<.0001	.9384

Intervention-C, interventional studies with complex complexity; Intervention-M, interventional studies with medium complexity; Intervention-S, interventional studies with simple complexity.

levels of this study to enable any pediatric or adult facility to model its population's size or other demographic characteristics (see Table 1), with RAK and DAP to produce alert levels as the foundation of a patient safety quality assurance program.

This study's fitted data provide numerous benefits for quality assurance programs including the development of target values of patient dose as a function of patient size unique to any facility. Just over half of the 31 US states that responded to a recent national survey currently require or plan to require recording of all patient radiation dose data for CCL procedures (Conference of Radiation Control Program Directors of the United States, unpublished results of a national survey). However, this is not a useful exercise if the reasonable levels of pediatric patient doses as a function of size are unknown. With the advent of RDIM and the results of this study, patient radiation doses can easily be collected and analyzed as part of a patient safety-centric quality assurance program; generally, an RDIM can be customized to create institution-specific alert level notifications.

In Figures 2 and Central Illustration, the RAK and DAP values relating to the 90th or 98th upper prediction boundary fitting functions identify patient doses that exceed 95% and 99% of all patient doses for a given patient size; when these alerts trigger in an RDIM, these cases should be investigated. The 50% upper prediction boundary corresponds to the RAK and DAP levels that may be compared with a national diagnostic reference level.[29] The fourth empirical fit labeled "linear" corresponds to the national achievable dose level.[30] No RAK or DAP for the diagnostic or intervention categories exceeded the level likely to produce skin effects, the typical threshold used for adult alert levels. Yet the RAK of 11 and 12 pediatric patients of all sizes in Figure 2A and Central Illustration, respectively exceeded the 99% level for similar patient size procedures. Investigations of these examinations may identify the cause of the elevated dose levels to help prevent similar reoccurrences. The importance of carefully monitoring and managing pediatric radiation doses to achieve levels substantially below skin effect thresholds is vital because 10% of the smallest pediatric patients with severe disease undergo multiple catheterizations during their lifetime.[2]

An adult quality assurance program might identify 2 alert levels, one for diagnostic and another for interventional examinations in an

Table 8. Published (Pub) vs this study's (Study) RAK and DAP.

Patient "Size"	Study complexity	Pub RAK[a] (mGy)	Study RAK[b] (mGy)	Percent reduction[c]	Pub DAP[a] (Gy·cm^2)	Study DAP[b] (Gy·cm^2)	Percent reduction[c]
< 1 y	Diagnostic	215	13	94%	7.43	1.7	77%
5-9 y	Diagnostic	291	24	92%	16.47	3.5	79%
>16 y	Diagnostic	1249	72	94%	82.84	12.5	85%
< 1 y	Intervention Low	197	9	95%	7.97	1.2	85%
< 1 y	Intervention Med	415	18	96%	13.8	2.5	82%
< 1 y	Intervention High	690	24	97%	22	3.3	85%
5-9 y	Intervention Low	421	18	96%	29	2.6	91%
5-9 y	Intervention Med	716	39	95%	48	6.5	86%
5-9 y	Intervention High	1446	50	97%	60	7.8	87%
>16 y	Intervention Low	1284	48	96%	92	11	88%
>16 y	Intervention Med	2080	143	93%	110	29	74%
>16 y	Intervention High	3994	126	97%	160	35	78%
< 1 y	Intervention Low	76	9	88%	5	1.2	76%
< 1 y	Intervention Med	122	18	85%	4	2.5	38%
< 1 y	Intervention High	137	24	82%	7	3.3	53%
5-9 y	Intervention Low	160	18	89%	13	2.6	80%
5-9 y	Intervention Med	244	39	84%	21	6.5	69%
5-9 y	Intervention High	444	50	89%	38	7.8	79%
>16 y	Intervention Low	949	48	95%	96	11	89%
>16 y	Intervention Med	882	143	84%	198	29	85%
>16 y	Intervention High	1716	126	93%	288	35	88%
< 5 kg	Diagnostic	29	6	79%	0.9	0.868	4%
< 5 kg	Intervention	26	18	31%	1.6	1.26	21%
15-30 kg	Diagnostic	52	17	67%	5	2.45	51%
15-30 kg	Intervention	118	38	68%	11.6	6.4	45%

Published data in rows 1 to 12[20]: frontal and lateral plane doses summed for published and study data to allow comparison.
Published date in rows 13 to 21[17]: published data are for single plane units; frontal and lateral plane doses of biplane study data summed.
Published data in rows 22 to 25[31]: published data are for single plane units; frontal and lateral plane doses of biplane study data summed.
DAP, dose area product; RAK, reference air KERMA.

[a] Pub RAK or Pub DAP: published RAK or DAP values. [b] Study RAK or Study DAP: RAK or DAP values from this study. [c] Percent reduction: (published dose – study dose)/published dose.

average-sized adult, but this is not adequate for pediatric patients. Dose alert levels for multiple groups stratified by median expected dose, (namely: 2 and 3 dose levels within diagnostic and interventional examinations, respectively) are necessary. These 5 different dose levels represent different procedural complexities leading to 5 different clinical models. Without these multiple dose level models, the smallest pediatric patients, who receive larger doses than necessary, would not be identified in a root cause analysis. The fitted intercepts of the 5 models are statistically significantly different (Table 7).

This study's patient RAK and DAP values can be scaled for use at a different facility by changing the fitted intercept values. Scaling these data allows adjustments for different models of fluoroscopic units, x-ray beam filtrations, tube voltages (ie, kV), tube current time products (ie, mAs), pulse widths, pulse rates, use or nonuse of antiscatter grids for smaller patients, air KERMA at the image receptor, the geometry of the fluoroscopes, skill level of operators, and complexity of procedures. The configuration of the fluoroscope needs to be adjusted by the manufacturer in consultation with cardiologists and qualified medical physicists at the facility to address the unique imaging requirements of each facility's fluoroscopic examinations.[9,10,27]

The calculations below illustrate how RAK or DAP alert levels may be calculated for different CCLs than those of the authors. A CCL's qualified medical physicist and staff can help manage and support many parts of a strong alert program by assisting with the following calculations. An adult facility should identify a minimum of 5 to 10 adult patients from whom the average patient size could be calculated. As an example of RAK and DAP alert level calculations, assume 10 patients, who underwent complex interventional procedures, had an average LAT of the thorax of 35 cm and average RAK and DAP values in the frontal and lateral planes of 100 mGy and 26,600 mGy·cm^2 and 175 mGy and 30,000 mGy·cm^2, respectively. The units of DAP vary per equipment manufacturer: μGy·m^2, Gym·m^2, cGy·cm^2, mGy·cm^2, etc. Displayed DAP values must be converted to mGy·cm^2 to be used with this publication's data. Substituting the 4 average doses (RAK_{avg} and DAP_{avg}), the average LAT (x_{avg}), and the appropriate slopes (m) from Tables 5 and 6 into Equation 3 allows the calculation of a modified fitted intercept ($\hat{c}$), where $\hat{c}$ transforms the data in this study to be applicable to that of a different facility:

RAK frontal plane: $\hat{c} = \ln(D_{avg}) - m \cdot x_{avg} = \ln(100) - 0.107 \cdot 35 = 0.8602$

DAP frontal plane: $\hat{c} = \ln(D_{avg}) - m \cdot x_{avg} = \ln(26,600) - 0.134 \cdot 35 = 5.499$

RAK lateral plane: $\hat{c} = \ln(D_{avg}) - m \cdot x_{avg} = \ln(175) - 0.139 \cdot 35 = 0.2998$

DAP lateral plane: $\hat{c} = \ln(D_{avg}) - m \cdot x_{avg} = \ln(30,000) - 0.167 \cdot 35 = 4.464$.

Where D_{avg} is either RAK_{avg} or DAP_{avg} in the above 4 calculations. The RAK and DAP alert levels for both the frontal and lateral planes based on the 98th upper prediction level can now be calculated for a 1-year-old with a 17 cm thick lateral projection using Equation 2 and coefficient data from Tables 5 and 6 as follows:

$$\hat{D}_{\alpha}(x_{new}) = EXP(m \cdot x_{new} + \hat{c} + s_{\alpha})$$

where $\hat{D}_{\alpha}(x_{new})$ is either RAK or DAP in the following calculations:

$RAK_{17\ cm}$ frontal plane $= EXP(0.107 \cdot 17 + 0.8602 + 2.384) = 158\ mGy$

DAP_{17cm} frontal plane $= EXP(0.134 \cdot 17 + 5.499 + 2.584) = 31,603\ mGy \cdot cm^2$

$RAK_{17\ cm}$ lateral plane $= EXP(0.139 \cdot 17 + 0.2998 + 2.16) = 124\ mGy$

$DAP_{17\ cm}$ lateral plane $= EXP(0.167 \cdot 17 + 4.464 + 2.207) = 13,494\ mGy \cdot cm^2$.

Each dose index (RAK or DAP) from the frontal and lateral planes cannot be summed because the dose from each gantry plane is required to properly manage patients with elevated doses and to avoid overestimating the patient's skin dose. These calculations represent the upper 99% threshold for babies with a thorax lateral dimension of 17 cm at an adult facility. In this example, an adult facility is a site that routinely examines patients over 21 years old but may in an emergent situation occasionally examine a patient less than 21 years old. In contrast, a pediatric facility routinely examines infants to 21-year-old patients (and even adults who are still being treated for their pediatric congenital disease) with lateral sizes from 10 cm to greater than 40 cm. The estimated doses (either RAK or DAP) for a 17 cm lateral-sized infant are higher than the original adult values because the original adult values are averages, while the estimated dose represents the top 1% of doses. Central Illustration shows that the top 1% of doses for a given patient size are about 10 times greater than the average dose. If average doses were estimated, the values for the infant would be lower than the original adult average doses.

Correlating RAK and DAP to the x-ray's path length through the patient's thorax, measured with calipers, is the best practice to scale this study's data to that of a different institution. However, the average LAT of the patient's thorax could be interpolated from data in Table 1 provided the weight, age, or BMI of the patient is known. The model may be used to assign an RAK and DAP alert level threshold for the frontal and lateral planes to each patient examination. If the RAK or DAP of either plane exceeds its alert level, the patient examination should be investigated. The results of the 2 planes for either RAK or DAP should not be summed.

Current pediatric patient's RAK and DAP values during cardiac catheterization procedures in the US as a function of measured LAT of the patient's thorax have not been previously published. Pediatric catheterization data from 2005-2009 from 1 US site was published by Verghese et al,[20] but patients were placed in only 5 different age groups. Ghelani et al[17] published similar data from 2009-2013 from 5 different US sites. De Monte et al[31] published 15 months of similar pediatric data, beginning in 2018, from 1 site in Italy; patients were grouped based on their mass. This study's data are compared to the 3 published studies in Table 8.[17,20,31] The reduction in dose of this study, compared to 10 years ago, ranged from 92% to 97% for RAK and 74% to 91% for DAP. This substantial improvement is due to imaging equipment design improvements and improved configuration for pediatric imaging as previously discussed. The dose reduction in this study was substantial vs Ghelani et al's[17] study due to the large time gap, ranging from 82% to 93% for RAK and 38% to 89% for DAP. Since the dates of the De Monte et al[31] study and this study overlap, the reductions are smaller, ranging from 31% to 79% for RAK and 4% to 51% for DAP.

This study has limitations. Multiple types of examinations are combined within the same patient groups to create larger sample sizes, in the case of our study greater than 450 (Table 4). The modeled RAK and DAP alert levels of this study require large sample sizes to ensure a reasonable representation of the larger pediatric population of the country. The average RAK of each procedural type independent of patient size is used to estimate the complexity of each type of category. The data from this single institution cannot be the sole basis for pediatric diagnostic reference levels or universal RAK and DAP alert levels. Although the patient's risk is more directly related to peak skin dose than RAK or DAP,[32] RAK and DAP provide a basis for qualified medical physicists to calculate other estimated patient doses, eg, dose to the heart, or other organ doses.

Conclusions

This study's fitted data scaled by its methodology allows the estimation of RAK and DAP alert levels for pediatric diagnostic and interventional procedures conducted in any pediatric CCL. The reduction in RAK from the largest to the smallest pediatric patient

can exceed an order of magnitude, signifying the need to stratify doses by patient size. Without this stratification, alert levels will be ineffectual for root cause analysis of excess doses to small patients. Pediatric interventional cardiac fluoroscopic alert levels as a function of the patient's LAT of the thorax should be used within a quality assurance program to verify appropriate patient care prior to, during, and after radiological examinations in the CCL.

Declaration of competing interest

The authors declared no potential conflicts of interest with respect to the research, authorship, and/or publication of this article.

Funding sources

This work was not supported by funding agencies in the public, commercial, or not-for-profit sectors.

Ethics statement and patient consent

The research reported in this study has adhered to all relevant ethical guidelines; the institutional review board waived the need for consent for this retrospective study.

References

1. Hoffman JIE, Kaplan S. The incidence of congenital heart disease. *J Am Coll Cardiol*. 2002;39(12):1890–1900. https://doi.org/10.1016/s0735-1097(02)01886-7
2. Wu W, He J, Shao X. Incidence and mortality trend of congenital heart disease at the global, regional, and national level, 1990-2017. *Medicine (Baltimore)*. 2020;99(23), e20593. https://doi.org/10.1097/MD.0000000000020593
3. Johnson JN, Hornik CP, Li JS, et al. Cumulative radiation exposure and cancer risk estimation in children with heart disease. *Circulation*. 2014;130(2):161–167. https://doi.org/10.1161/CIRCULATIONAHA.113.005425
4. Mettler FA, Mahesh M, Chatfield MB, et al. *Report No. 184 – Medical Radiation Exposure of Patients in the United States*. National Council on Radiation Protection and Measurements; 2019. Accessed February 17, 2024. https://ncrponline.org/shop/reports/report-no-184-medical-radiation-exposure-of-patients-in-the-united-states-2019/
5. Lang NN, Walker NL. Adult congenital heart disease and radiation exposure: the malignant price of cardiac care. *Circulation*. 2018;137(13):1346–1348. https://doi.org/10.1161/CIRCULATIONAHA.117.032815
6. Haas NA, Happel CM, Mauti M, et al. Substantial radiation reduction in pediatric and adult congenital heart disease interventions with a novel X-ray imaging technology. *Int J Cardiol Heart Vasc*. 2015;6:101–109. https://doi.org/10.1016/j.ijcha.2015.01.007
7. Christopoulos G, Makke L, Christakopoulos G, et al. Optimizing radiation safety in the cardiac catheterization laboratory: a practical approach. *Catheter Cardiovasc Interv*. 2016;87(2):291–301. https://doi.org/10.1002/ccd.25959
8. Gutiérrez-Barrios A, Camacho-Galán H, Medina-Camacho F, et al. Effective reduction of radiation exposure during cardiac catheterization. *Tex Heart Inst J*. 2019;46(3):167–171. https://doi.org/10.14503/THIJ-17-6548
9. Strauss KJ. Pediatric interventional radiography equipment: safety considerations. *Pediatr Radiol*. 2006;36(Suppl 2):126–135. https://doi.org/10.1007/s00247-006-0220-4
10. Strauss KJ. Advancing safety: role of equipment design and configuration change in pediatric fluoroscopy. *Health Phys*. 2019;116(2):256–262. https://doi.org/10.1097/HP.0000000000001002
11. Liu B, Hirsch JA, Li X, et al. Radiation dose monitoring for fluoroscopically guided interventional procedures: effect on patient radiation exposure. *Radiology*. 2019;290(3):744–749. https://doi.org/10.1148/radiol.2019180799
12. Rehani MM. Patient radiation exposure and dose tracking: a perspective. *J Med Imaging (Bellingham)*. 2017;4(3), 031206. https://doi.org/10.1117/1.JMI.4.3.031206
13. Zucca S, Solla I, Boi A, et al. The role of a commercial radiation dose index monitoring system in establishing local dose reference levels for fluoroscopically guided invasive cardiac procedures. *Phys Med*. 2020;74:11–18. https://doi.org/10.1016/j.ejmp.2020.04.019
14. Osei B, Xu L, Johnston A, Darko S, Darko J, Osei E. Retrospective study of patients radiation dose during cardiac catheterization procedures. *Br J Radiol*. 2019;92(1099), 20181021. https://doi.org/10.1259/bjr.20181021
15. Bacher K, Bogaert E, Lapere R, De Wolf D, Thierens H. Patient-specific dose and radiation risk estimation in pediatric cardiac catheterization. *Circulation*. 2005;111(1):83–89. https://doi.org/10.1161/01.CIR.0000151098.52656.3A
16. Boothroyd A, McDonald E, Moores BM, Sluming V, Carty H. Radiation exposure to children during cardiac catheterization. *Br J Radiol*. 1997;70:180–185. https://doi.org/10.1259/bjr.70.830.9135445
17. Ghelani SJ, Glatz AC, David S, et al. Radiation dose benchmarks during cardiac catheterization for congenital heart disease in the United States. *JACC Cardiovasc Interv*. 2014;7(9):1060–1069. https://doi.org/10.1016/j.jcin.2014.04.013
18. Li LB, Kai M, Kusama T. Radiation exposure to patients during paediatric cardiac catheterisation. *Radiat Prot Dosimetry*. 2001;94(4):323–327. https://doi.org/10.1093/oxfordjournals.rpd.a006506
19. Martin EC, Olson A. Radiation exposure to the paediatric patient from cardiac catheterization and angiocardiography. *Br J Radiol*. 1980;53(626):100–106. https://doi.org/10.1259/0007-1285-53-626-100
20. Verghese GR, McElhinney DB, Strauss KJ, Bergersen L. Characterization of radiation exposure and effect of a radiation monitoring policy in a large volume pediatric cardiac catheterization lab. *Catheter Cardiovasc Interv*. 2012;79(2):294–301. https://doi.org/10.1002/ccd.23118
21. Balter S, Moses J. Managing patient dose in interventional cardiology. *Catheter Cardiovasc Interv*. 2007;70(2):244–249. https://doi.org/10.1002/ccd.21141
22. Kleinman PL, Strauss KJ, Zurakowski D, Buckley KS, Taylor GA. Patient size measured on CT images as a function of age at a tertiary care children's hospital. *AJR Am J Roentgenol*. 2010;194(6):1611–1619. https://doi.org/10.2214/AJR.09.3771
23. Fryar CD, Kruszon-Moran D, Gu Q, Carroll M, Ogden CL. Mean body weight, height, waist circumference, and body mass index among children and adolescents: United States, 1999–2018. *National Health Statistics Reports*. 2021;160. Accessed August 1, 2024. https://www.cdc.gov/nchs/data/nhsr/160-508.pdf
24. Lin PJ, Schueler BA, Balter S, et al. Accuracy and calibration of integrated radiation output indicators in diagnostic radiology: a report of the AAPM Imaging Physics Committee Task Group 190. *Med Phys*. 2015;42(12):6815–6829. https://doi.org/10.1118/1.4934831
25. Emmeans: estimated marginal means, aka least-squares means. R package version 1.4.7. Accessed December 24, 2023. https://rvlenth.github.io/emmeans/.
26. *R: A language and environment for statistical computing*. R Foundation for Statistical Computing; 2023. Accessed January 17, 2024. https://www.r-project.org./
27. Somasundaram E, Brady SL, Strauss KJ. Application of reference air kerma alert levels for pediatric fluoroscopic examinations. *J Appl Clin Med Phys*. 2022;23(9), e13721. https://doi.org/10.1002/acm2.13721
28. Kirkwood BR, Sterne JAC. *Essential Medical Statistics*. 2nd ed. Wiley-Blackwell; 2003.
29. Vañó E, Miller DL, Martin CJ, et al. ICRP Publication 135: diagnostic reference levels in medical imaging. *Ann ICRP*. 2017;46(1):1–144. https://doi.org/10.1177/0146645317717209
30. Brink JA, Boone JM, Feinstein KA, et al. *Report No. 172 – Reference levels and achievable doses in medical and dental imaging: recommendations for the United States*. National Council on Radiation Protection and Measurements; 2012. Accessed January 16, 2024. https://ncrponline.org/shop/reports/report-no-172-reference-levels-and-achievable-doses-in-medical-and-dental-imaging-recommendations-for-the-united-states-2012/
31. De Monte F, Castaldi B, Branchini M, et al. Typical values for pediatric interventional cardiology catheterizations: a standardized approach towards diagnostic reference level establishment. *Phys Med*. 2020;76:134–141. https://doi.org/10.1016/j.ejmp.2020.07.001
32. Fletcher DW, Miller DL, Balter S, Taylor MA. Comparison of 4 techniques to estimate radiation dose to skin during angiographic and interventional radiology procedures. *J Vasc Interv Radiol*. 2002;13(4):391–397. https://doi.org/10.1016/s1051-0443(07)61742-4